

Zero-Shot Generalization for Blockage Localization in mmWave Communication

Rafaela Scaciota^{*†}, *Member, IEEE*, Malith Gallage^{*}, *Student Member, IEEE*, Sumudu Samarakoon^{*†}, *Member, IEEE*, and Mehdi Bennis^{*}, *Fellow, IEEE*

^{*}Centre for Wireless Communication, University of Oulu, Finland

[†]Infotech Oulu, University of Oulu, Finland

email: {rafaela.scaciotatimoedasilva, malith.gallage, sumudu.samarakoon, mehdi.benni}@oulu.fi

Abstract—This paper introduces a novel method for predicting blockages in millimeter-wave (mmWave) communication systems towards enabling reliable connectivity. It employs a self-supervised learning approach to label radio frequency (RF) data with the locations of blockage-causing objects extracted from light detection and ranging (LiDAR) data, which is then used to train a deep learning model that predicts object’s location only using RF data. Then, the predicted location is utilized to predict blockages, enabling adaptability without retraining when transmitter-receiver positions change. Evaluations demonstrate up to 74% accuracy in predicting blockage locations in dynamic environments, showcasing the robustness of the proposed solution.

Index Terms—Radio Frequency, mmWave, Localization, LiDAR, Deep learning.

I. INTRODUCTION

Millimeter-wave (mmWave) communication has emerged as a promising technology for next-generation wireless networks due to its ability to offer high data rates with low latency. However, mmWave signals are susceptible to blockages caused by objects in the environment, which can lead to signal attenuation and link failures [1]. Therefore, predicting and mitigating blockages in mmWave communication systems have become critical to ensure reliable and uninterrupted connectivity. Anticipating the blockages in advance allows proactive measures to maintain signal integrity and enhance quality of service (QoS) through mechanisms such as handover, beamforming, caching, and others [2].

The recent advancements in wireless communication technologies, especially in the mmWave bands, have significant research interest in blockage prediction. Building on the foundational propagation models and performance metrics for 5G mmWave bands established in [3], researchers have explored innovative applications of mmWave technology beyond traditional communication. For example, [4] showcased the use of mmWave radar for indoor object detection and tracking, while [5] introduced multimodal split learning techniques to improve mmWave received power prediction in resource-constrained settings. Expanding further, [6] utilized light detection and ranging (LiDAR) to predict mobile blockages and optimize beam computation, and [7] proposed advanced learning techniques such as distributed heteromodal split learn-

ing and self-supervised radio-visual representation learning to refine prediction and sensing capabilities. Together, these advancements underscore the potential of integrating diverse sensing modalities to enhance the robustness and functionality of mmWave communication systems.

The application of mmWave and multisensor technologies goes beyond traditional communication paradigms. In [8], a self-supervised geometric learning framework for automatic Wi-Fi human sensing is introduced for internet of things (IoT) applications. Furthermore, the authors in [9] explored self-supervised federated learning approaches for multisensor representations, offering scalable and privacy-preserving embedded intelligence solutions in various sensor networks. In [10], the authors use LiDAR sensory data to detect whether an object will block the mmWave communication link between transmitter (Tx) and receiver (Rx). The authors in [11] use a deep learning architecture proposed to learn the pre-blockage signal in the radio frequency (RF) and LiDAR data and successfully predict blockages proactively. One drawback of the previous studies is that even a slight change in the position of the Tx or Rx requires the model to be re-trained and thus, developing robust and adaptive blockage prediction techniques are paramount for mmWave communication system designs.

The main contribution of this paper is to propose a **novel blockage prediction solution for mmWave communication systems using stressing cross-self-supervised learning (SSL)** that can be easily adapted for certain modifications in the environments. Towards this, we first employ a SSL approach to label the RF data with the locations of objects causing the blockages that are extracted from LiDAR data. Using them, we train a long short-term memory (LSTM) neural network to predict future object locations. Then, a geometric analysis is carried out to evaluate whether a blockage will occur at the predicted location at any given time. The proposed solution can be used to predict the blockages at newly deployed Tx-Rx links in the vicinity, by simply reconfiguring the geometric analysis without a need of retraining the deep learning (DL) model. Finally, we present a real-world evaluation of a point-to-point communication scenario using the deepSense6G dataset [12]. This paper is organized as follows. Section II presents the system model and the problem formulation. The

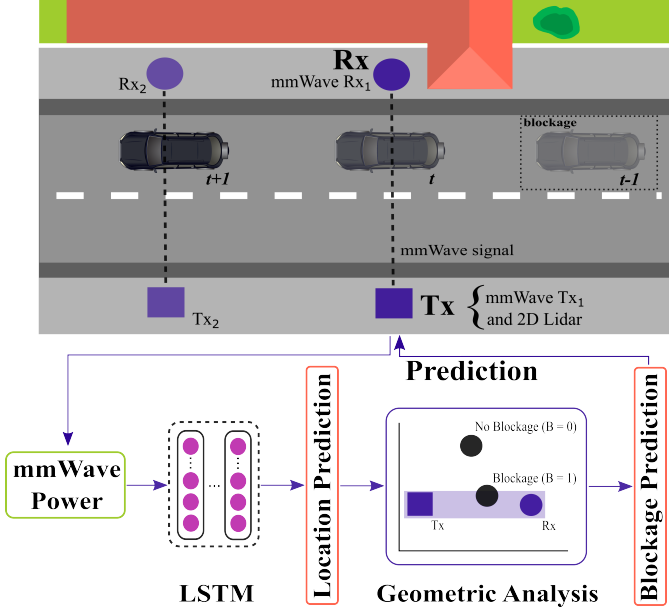


Figure 1: Top: Overall system model where a mmWave base station leverages both LiDAR and in-band wireless sensing to predict the object location coordinates. Bottom: The flow diagram highlighting the key steps of the proposed solution.

methodology is discussed in Section III. Section IV lays out the evaluation of the proposed method while Section V draws the conclusions.

II. SYSTEM MODEL & PROBLEM FORMULATION

We consider a point-to-point mmWave communication system consisting of a Tx M_A -element uniform linear array (ULA) antenna and a static Rx with a single antenna. The Tx is equipped with a 2D LiDAR that provides situational awareness about the environment and any moving objects, as shown in Fig. 1. The system uses a predetermined beam steering codebook consisting of M beams, denoted as $\mathcal{F} = \{\mathbf{f}_m\}_{m=1}^M$. Each beam steering vector $\mathbf{F}_m = \mathbf{f}_m(\Theta_m)$ is designed to direct signals in a specific direction given by $\Theta_m = \Theta_{\text{offset}} + (F_{\text{off-view}}/M)$, where Θ_{offset} is the signal direction offset and, $F_{\text{off-view}}$ denotes the field-of-view (FoV) of the wireless beamforming system.

The signal transmission model is orthogonal frequency-division multiplexing (OFDM) with K subcarriers. We denote $\mathbf{h}_{k,t} \in \mathbb{C}^{M \times 1}$ as the downlink channel from Tx to Rx on the k^{th} subcarrier at time t , where $t \in \mathbb{Z}$. At time t , if the Tx adopts the beam steering vector \mathbf{F}_m for downlink transmission, the received signal at subcarrier k is represented as

$$r_{k,m,t} = \mathbf{h}_{k,t}^T \mathbf{F}_m s_{k,t} + n_{k,t}, \quad (1)$$

where $s_{k,t}$ represents the transmitted symbol at the k^{th} subcarrier with $\mathbb{E}[s_{k,t}^2] = 1$, and $n_{k,t} \sim \mathcal{CN}(\mathbf{0}, \sigma_n^2)$ is complex Gaussian noise with zero mean and the covariance of σ_n^2 . In this view, the received signal strength indicator (RSSI) vector of the M beams at time t can be defined as $\mathbf{r}_t =$

$[|r_{1,t}|^2, \dots, |r_{M,t}|^2]^T \in \mathcal{S}$, where \mathcal{S} is the RSSI observation space, and $|r_{m,t}|^2 = \sum_{k=1}^K |r_{k,m,t}|^2$ represents the total power received by the m^{th} beamforming vector over K subcarriers. We assume that a collection $\mathbf{S}_t = [\mathbf{r}_{t-\tau}]_{\tau \in \mathcal{T}} \in \mathcal{S}^{T_0}$ of past T_0 RSSI observations are drawn from a bounded space where $\mathcal{T} = \{0, 1, \dots, T_0\}$.

Simultaneously, the LiDAR sensor in Tx provides a snapshot of the surrounding environment at each time step t through a data matrix $\ell_t \in \mathcal{L}$ where \mathcal{L} defines the LiDAR observation space. Each row represents a single LiDAR point characterized by the angle related to the sensor and the depth value measured at the corresponding angle. Similar to RSSI, we define a collection of T_0 past LiDAR observations at time t as $\mathbf{L}_t = [\ell_{t-\tau}]_{\tau \in \mathcal{T}} \in \mathcal{L}^{T_0}$.

In a mmWave communication setting, a blockage is defined by an event where the resultant signal strength at the Rx over K subcarriers is below a predefined threshold r_0 . In this view, we formally define an indication of a blockage at a given time t as $b_t = \mathbb{1}(|r_t| < r_0)$ where $\mathbb{1}(\cdot)$ is the indicator function. The conventional data-driven designs of blockage predictions over a future horizon of length N rely on the past sensory information by learning a mapping function $U_\theta : \mathcal{S}^{T_0} \times \mathcal{L}^{T_0} \rightarrow \{0, 1\}^N$ with parameters θ . Therein, the learning objective can be formalized as follows:

$$\min_{\theta} \lim_{T \rightarrow \infty} \frac{1}{T} \sum_{t=0}^T \frac{\|U_\theta(\mathbf{S}_t, \mathbf{L}_t) - \boldsymbol{\rho}_t\|^2}{N}, \quad (2)$$

where $\hat{\boldsymbol{\rho}}_t = [\hat{b}_{t+1}, \dots, \hat{b}_{t+N}]$ and $\boldsymbol{\rho}_t = [b_{t+1}, \dots, b_{t+N}]$ are the predicted and actual future blockages, respectively.

In contrast to exploiting the correlation between RSSI, LiDAR data and blockage, we seek a method to utilize the dependencies of sensory data and object locations to predict future locations of the object and derive future blockages based on the geometry of Tx-Rx link and object locations. It is worth noting that the object location is unavailable and, thus, needs to be extracted from a mapping $V_\phi : \mathcal{L} \rightarrow \mathcal{X}$ with parameter ϕ in a self-supervised manner. Here, \mathcal{X} represents the space of the object locations. Then, the future locations for N time horizon can be predicted via learning a ψ -parametric function $W_\psi : \mathcal{X} \times \mathcal{S}^{T_0} \rightarrow \mathcal{X}^N$. Learning W_ψ is carried out with the following objective:

$$\min_{\phi, \psi} \lim_{T \rightarrow \infty} \frac{1}{T} \sum_{t=0}^T \frac{\Gamma(W_\psi(\mathbf{S}_t, V_\phi(\ell_t)), \boldsymbol{\gamma}_t)}{N}, \quad (3)$$

where $\boldsymbol{\gamma}_t = [V_\phi(\ell_{t+\tau})]_{\tau \in \{1, \dots, N\}}$ is the future locations of the object, and Γ is the loss function.

III. DEEP LEARNING SOLUTION FOR BLOCKAGE PREDICTION

The problem described in (3) can be cast as a deep learning problem due to the inherent capability to model complex, non-linear relationships in data. In this context, the goal is to understand the relationships between object locations and blockage events, making it well-suited for analyzing blockage

dynamics and predicting future blockages based on the past observations.

To predict future blockages, our deep learning approach comprises two stages: (i) creating a labeled dataset of RSSI and location data through SSL and (ii) implementing the deep learning solution to predict blockages based on object location. The experimental setup used to evaluate the proposed deep learning solution, including the mmWave communication system and the associated testbed, was developed by the deepSense6G project [12].

A. Self-supervised approach for dataset generation

To improve data quality and isolate relevant information, we applied the static clutter removal (SRC) noise filtering algorithm to the raw LiDAR data as proposed by the authors in [13]. We filter out potential noise by removing the LiDAR points within a defined proximity to Tx and isolate the road section by removing all other surrounding data. This ensures that we filter out the LiDAR points that do not belong to objects on the road.

Then, we employ an unsupervised learning approach to label RF data, allowing the grouping of LiDAR data points into distinct categories based on their similarities to estimate the location of the object as $\gamma_t = V_\phi(\ell_t)$. We apply the density-based spatial clustering of applications with noise (DBSCAN) unsupervised learning framework, which is known for its ability to cluster data points densely packed in high-density regions [14]. The dataset is generated with the collection of T_0 such observations, which is denoted by $\mathcal{D} = \{(\mathbf{S}_t, \gamma_t)\}_{t \in \{1, \dots, T_0\}}$.

B. Blockage Prediction based on Object Location

First, we predict the future locations of the object by learning the mapping W_ψ using a deep learning model. Among the most efficient types of deep learning for activity prediction, LSTM stands out due to its unique ability to remember single events over long and often unknown periods. Here, the LSTM output is a scalar representing the object location. During the training period, given the fixed length of the observation window T_i , let $\mathbf{I}_t = [(\mathbf{S}_t, \gamma_t), \dots, (\mathbf{S}_{t-T_i+1}, \gamma_{t-T_i+1})]$, denote an input data sample. As for the loss function, we use smooth mean absolute error (sMAE), also known as Huber Loss, given by

$$\Gamma(\mathbf{Z}_t) = \begin{cases} \frac{1}{2} \mathbf{Z}_t^2, & \text{if } |\mathbf{Z}_t| \leq \delta, \\ \delta(|\mathbf{Z}_t| - \frac{1}{2}\delta), & \text{otherwise,} \end{cases} \quad (4)$$

where $\mathbf{Z}_t = W_\psi(\mathbf{I}_t) - \gamma_t$, and $\delta \in \mathbb{R}^+$ is the parameter that determines the threshold for switching between the quadratic and linear components of the loss function. This makes the function less sensitive to outliers, but it also leads to penalization of minor errors within the data sample. Adam optimizer obtains the optimal choices for ϕ and ψ . Finally, to predict the blockage, we apply a geometric analysis that incorporates the vehicle location as

$$B_t = \begin{cases} 1, & \text{if } 0 \leq v \leq 1 \text{ and } 0 \leq u \leq 1, \\ 0, & \text{otherwise,} \end{cases} \quad (5)$$

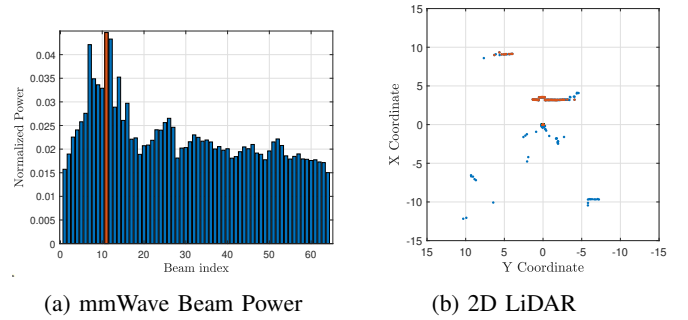


Figure 2: DeepSense 6G dataset visualization. a) Blue bar: average RSSI over the 16×16 beams. Red bar: the RSSI of an arbitrarily selected beam. b) Blue points: raw LiDAR data. Red points: isolated relevant LiDAR data.

Parameter	RF Blockage	Lidar + RF Blockage	RF Localization
	Value		
Input size	64	64	64
Hidden Size	16	16	32
LSTM Layers	4	2	1
Learning rate	$1e-3$	$1e-3$	$1e-3$
Batch size	8	8	8
Loss function	BCE Loss	BCE Loss	Huber Loss
Episodes	10		
Iterations	100		

Table I: Deep neural network (DNN) model parameters.

where $v = (\hat{y}_B - y_T)/(y_R - y_T)$ and $u = 1/2 + (1/\omega)(\hat{x}_B - y_T - t)$. Here, the predicted object location is $\hat{\gamma}_t = (\hat{x}_B, \hat{y}_B)$, the object width is ω , and the locations of Tx and Rx are (x_T, y_T) and (x_R, y_R) , respectively.

IV. PERFORMANCE EVALUATION

For the evaluations, we rely on the data from the deepSense6G project [12], a large-scale data set that captures real-world LiDAR, communication, and positional data for research. More specifically, we adopt the scenarios 24 – 29 in deepSense6G testbed 3 to create the dataset. The testbed 3 features a Tx and a Rx, each equipped with 60 GHz mmWave phased arrays consisting of 16-element ULA. The communication uses OFDM modulation with a bandwidth of 20 MHz and 64 subcarriers. The LiDAR is mounted on the Tx. The scanning range of LiDAR is 16 meters and the motor spin frequency is 10Hz. At each capture, LiDAR creates a 360° point cloud.

A snapshot of data used in this work is presented in Fig. 2. Fig. 2a shows the average RSSI over the 16×16 beams as the blue bar and the red bar is the RSSI of an arbitrarily selected beam. The bird's eye view constructed using the 2D LiDAR data is presented in Fig. 2b. Here, the raw data from LiDAR is shown as blue points, and the isolated relevant LiDAR data is shown in red.

To structure the data prepared for vehicle location prediction, we used a sliding window method with an observation window size of $T_0 = 8$. The sequenced data were then used to train a LSTM network to predict the location of the vehicle centroids for the following $N = 5$ time windows. We used a distance threshold of $\epsilon = 2$ to determine the neighbor relationships between points to cluster data points. Furthermore, we established a minimum sample size of 4 points required to form a cluster.

The LSTM is configured with a hidden layer that determines the dimensionality of its hidden state. The output of the LSTM layers is arranged so that the batch size is the first dimension, which is then processed through two fully connected (dense) layers. The first dense layer reduces the dimensionality from 64 to 20 neurons and applies a rectified linear unit (ReLU) activation function to introduce non-linearity. The output of this layer is passed to the second dense layer, which further reduces the output to $2N$ neurons. A final ReLU activation function is applied to produce the final output. We denote the proposed framework as **RF-Localization** to explicitly indicate that the proposed framework utilizes received power values for the localization prediction, then evaluate the blockage applying (4).

The proposed prediction framework is evaluated against two baseline models that rely exclusively on either RSSI sequences and/or LiDAR sequences. In the first baseline model, referred to as **RF-Blockage**, only the RSSI values are fed into the LSTM layer. This model uses the same architecture as the **RF-Localization** model; however, the labels are the blockage states and evaluated with a binary cross-entropy (BCE) loss. Then, the blockage event needs to be extracted from a mapping as $H_\phi : \mathcal{L} \rightarrow \mathcal{B}$ with parameter ϕ in a self-supervised manner. Here, \mathcal{B} represents the space of the blockage events. As a result, the model learns a mapping function, $U_\theta : \mathcal{S}^{T_0} \times H_\phi(\ell_t) \rightarrow \{0, 1\}^N$, where the output represents the predicted blockage states

In the second baseline, termed as **RF+LiDAR-Blockage**, we also predicted blockage states using a multimodal framework that utilizes both LiDAR and RSSI values for the prediction by learning a mapping function $U_\theta : \mathcal{S}^{T_0} \times \mathcal{L}^{T_0} \rightarrow \{0, 1\}^N$. The multimodal framework integrates two components: a convolutional neural network (CNN) and a LSTM. The CNN processes LiDAR data, leveraging convolutional layers to extract spatial features and patterns. Meanwhile, the LSTM analyzes sequential RF data, capturing temporal dependencies. The outputs from these two networks are concatenated into a unified feature vector, which merges both spatial and temporal information. This combined vector is then fed into a fully connected layer that transforms it into a final output of size $2N$. To produce the final predictions, a sigmoid activation function is applied to the output, generating probability values that can be interpreted as the model’s predictions. It is worth highlighting that **RF+Lidar-Blockage** model is evaluated with a BCE loss.

The model parameters and hyperparameters used in this work are presented in Table I, unless specified otherwise. The

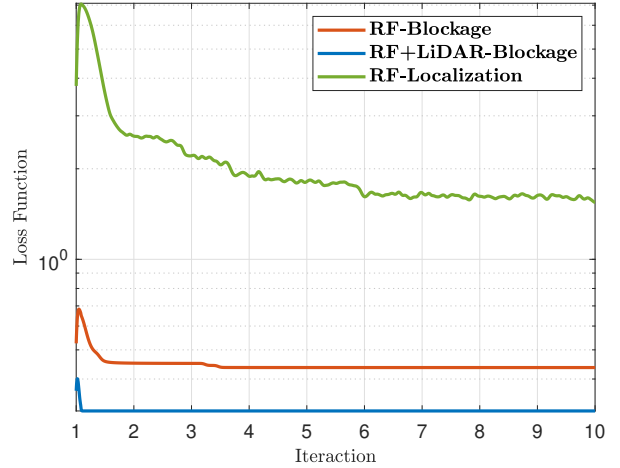


Figure 3: Training loss LSTM model using **RF-Blockage** method, **RF+LiDAR-Blockage** method and the proposed method, **RF-Localization**.

dataset was divided into three parts: training data for model training, validation data to check for possible overfitting and accordingly tune hyperparameters, and test data for performance evaluations.

We begin by examining the convergence behavior of the DNN during the training and validation phases to address the risk of significant overfitting. First, we analyze the convergence of trained models with three methods in Fig. 3. It shows that the **RF-Localization** method has a slower convergence compared to **RF-Blockage** and **RF+Lidar-Blockage**, potentially due to the high randomness observed in its only input: RSSI data. Note that the loss for **RF-Localization** is related to the location of the vehicle, whereas for **RF-Blockage** and **RF+Lidar-Blockage**, the loss is associated with the detection of blockages.

The model’s performance is evaluated using the blockage prediction accuracy shown in Fig. 4. The proposed solution achieved an accuracy of approximately 74.47% and a precision of approximately 86.96%. In comparison, the baseline methods **RF-Blockage** and **RF+Lidar-Blockage** have accuracies of approximately 93, 60% and 98.52%, respectively. Fig. 4 shows blockage prediction accuracy across different prediction horizons, with values generally clustered around 63–85%. The error bars indicate variability, with longer horizons displaying greater uncertainty in prediction accuracy, although the central trend remains relatively stable. Note that the variability of the baseline methods increases with the prediction horizon, while the variability of the proposed method remains stable.

In Fig. 5, we consider blockage prediction at a newly introduced Tx-Rx link without end-to-end retraining. This demonstrates a fundamental limitation of baseline methods like **RF-Blockage** and **RF+Lidar-Blockage**, which require extensive retraining to adapt to new Tx-Rx configurations. In contrast, our method employs a consistent prediction strategy:

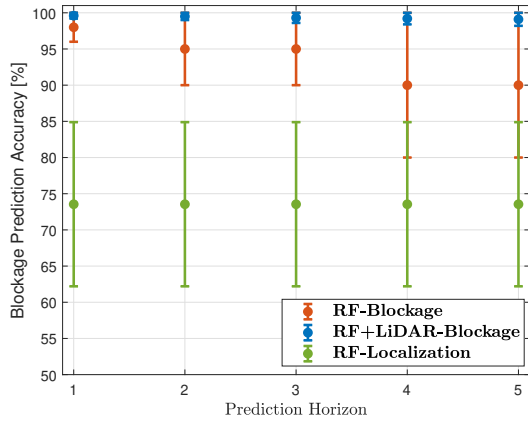


Figure 4: Blockage prediction accuracy using **RF-Blockage** method, **RF+LiDAR-Blockage** method and the proposed method, **RF-Localization**.

it first estimates vehicle centroids' locations and then determines blockage likelihood through geometric analysis. This highlights the generalizability and adaptability of our approach across different Tx-Rx pairs, sacrificing a certain degree of prediction accuracy, as observed in Fig. 4.

Fig. 5 also compares vehicle centroids' actual and predicted locations over various time windows using the scenario dataset 27. The close alignment of trajectories illustrates the precision of our model. Furthermore, using the same trained model, we showcase the ability to identify blockage events across multiple Tx-Rx pairs. By decoupling location prediction from blockage evaluation, our proposed method provides flexibility, requiring only adjustments in geometric analysis for new configurations, thereby avoiding the costly retraining needed by baseline methods.

V. CONCLUSION

In this paper, we introduced a novel approach for predicting blockages in mmWave communication systems using self-supervised learning and deep learning on RF and LiDAR data. Our method first labels RF data with object locations using LiDAR data as input for a DBSCAN algorithm and then applies an LSTM model to predict location events based solely on the labeled RF data. Then, we apply the predicted location in a geometric analysis to verify if the blockages occur. Real-world evaluations using the deepSense6G dataset showed that our model can correctly identify over 74% of blockages, with 86% of positive predictions being accurate. A key strength of this approach is its ability to preemptively identify blockage events and use that information at the transmitter for proactive decision-making, without requiring retraining, in which the same model can also be applied to predict blockages for other Tx-Rx links in the surrounding area.

REFERENCES

[1] T. S. Rappaport, Y. Xing, G. R. MacCartney, A. F. Molisch, E. Mellios, and J. Zhang, "Overview of millimeter wave communications for fifth-

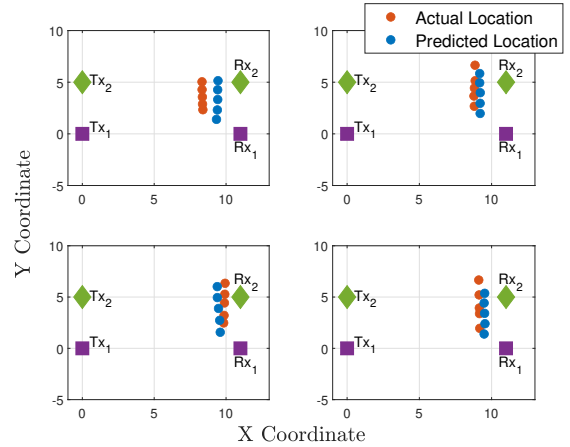


Figure 5: Actual and predicted 5 subsequent locations of the vehicle centroids for different time windows.

generation (5G) wireless networks—with a focus on propagation models," *IEEE Transactions on Antennas and Propagation*, vol. 65, no. 12, pp. 6213–6230, 2017.

[2] H. Yang, W.-D. Zhong, C. Chen, A. Alphones, and P. Du, "QoS-driven optimized design-based integrated visible light communication and positioning for indoor IoT networks," *IEEE Internet of Things Journal*, vol. 7, no. 1, pp. 269–283, 2020.

[3] S. Sun, T. S. Rappaport, M. Shafi, P. Tang, J. Zhang, and P. J. Smith, "Propagation models and performance evaluation for 5G millimeter-wave bands," *IEEE Transactions on Vehicular Technology*, vol. 67, no. 9, pp. 8422–8439, 2018.

[4] X. Huang, J. K. P. Tsoi, and N. Patel, "mmWave radar sensors fusion for indoor object detection and tracking," *Electronics*, vol. 11, no. 14, 2022.

[5] Y. Koda, J. Park, M. Bennis, K. Yamamoto, T. Nishio, M. Morikura, and K. Nakashima, "Communication-efficient multimodal split learning for mmwave received power prediction," *IEEE Communications Letters*, vol. 24, no. 6, pp. 1284–1288, 2020.

[6] S. Jiang, G. Charan, and A. Alkhateeb, "LiDAR aided future beam prediction in real-world millimeter wave V2I communications," *IEEE Wireless Communications Letters*, vol. 12, no. 2, pp. 212–216, 2023.

[7] M. Alloulah, A. D. Singh, and M. Arnold, "Self-supervised radio-visual representation learning for 6G sensing," in *ICC 2022 - IEEE International Conference on Communications*, 2022, pp. 1955–1961.

[8] J. Yang, X. Chen, H. Zou, D. Wang, and L. Xie, "AutoFi: Toward automatic Wi-Fi human sensing via geometric self-supervised learning," *IEEE Internet of Things Journal*, vol. 10, no. 8, pp. 7416–7425, 2023.

[9] A. Saeed, F. D. Salim, T. Ozcelebi, and J. Lukkien, "Federated self-supervised learning of multisensor representations for embedded intelligence," *IEEE Internet of Things Journal*, vol. 8, no. 2, pp. 1030–1040, 2021.

[10] S. Wu, C. Chakrabarti, and A. Alkhateeb, "Proactively predicting dynamic 6G link blockages using LiDAR and in-band signatures," *IEEE Open Journal of the Communications Society*, vol. 4, pp. 392–412, 2023.

[11] —, "LiDAR-aided mobile blockage prediction in real-world millimeter wave systems," in *2022 IEEE Wireless Communications and Networking Conference (WCNC)*, 2022, pp. 2631–2636.

[12] A. Alkhateeb, G. Charan, T. Osman, A. Hredzak, J. Morais, U. Demirhan, and N. Srinivas, "Deepsense 6G: A large-scale real-world multi-modal sensing and communication dataset," *IEEE Communications Magazine*, 2023.

[13] S. Wu, C. Chakrabarti, and A. Alkhateeb, "LiDAR-aided mobile blockage prediction in real-world millimeter wave systems," in *2022 IEEE Wireless Communications and Networking Conference (WCNC)*, 2022, pp. 2631–2636.

[14] M. Ester, H.-P. Kriegel, J. Sander, X. Xu *et al.*, "A density-based algorithm for discovering clusters in large spatial databases with noise," in *kdd*, vol. 96, no. 34, 1996, pp. 226–231.